Examining the effect of chronic intranasal oxytocin administration on the neuroanatomy and behavior of three autism-related mouse models

Zsuzsa Lindenmaier[1,2], Jacob Ellegood[1], Monique Stuvie[1], Kaitlyn Easson[1], Jane Foster[3], Evdokia Anagnostou[4], Jason P. Lerch[1,2,5]

[1]Mouse Imaging Centre, Hospital for Sick Children, Toronto, Ontario, Canada

[2]Department of Medical Biophysics, University of Toronto, Toronto, Ontario, Canada

[3]Department of Psychiatry and Behavioral Neurosciences, McMaster University, St.Joseph's Healthcare, Hamilton, Ontario, Canada

[4]Autism Research Center, Holland Bloorview Kids Rehabilitation Hospital, Toronto, Canada

[5]Wellcome Centre for Integrative NeuroImaging, University of Oxford, Oxford, United Kingdom

Abstract

Due to the heterogeneous nature of autism, treatment will likely only ameliorate symptoms in a subset of patients. To determine what might contribute to response susceptibility, we chronically treated the *16p11.2* deletion, *Shank3* (exon 4-9) knockout, and *Fmr1* knockout mouse models with intranasal oxytocin. Intranasal oxytocin was administered daily, for 28 days, starting at 5 weeks of age. The behavior of the mice was assessed in multiple domains: repetitive behaviors (as assessed by grooming), sociability (three chamber sociability task), anxiety and hyperactivity (open field), and learning and motor coordination (rotarod). The mice underwent three *in vivo* longitudinal MRI scans and a final high resolution *ex vivo* scan to assess the changes in neuroanatomy in response to treatment. No significant effect of treatment was found on social behavior in any of the strains, although a significant effect of treatment was found in the *Fmr1* mouse, with treatment normalizing a grooming deficit. No other treatment effect on behavior was observed that survived multiple comparisons correction. Treatment effect on the neuroanatomy did not reach significance. Overall, chronic treatment with oxytocin had limited and modest effects on the three mouse models related to autism, and no promising pattern of response susceptibility emerged.

1 Introduction

Autism spectrum disorder (ASD) is a very heterogeneous neurodevelopmental disorder, characterized by impaired social communication and repetitive behaviors. To date, there is no pharmacological treatment to improve the social/communication deficits in autism patients.[1,2] One promising pharmacological treatment for these social communication deficits is oxytocin.

Oxytocin is a neuromodulator, used in humans commercially to induce labor, but is known for its social effects. Clinical trials have shown that oxytocin induces anxiolytic and anti-depressant effects, to promote social recognition.[3] Oxytocin also leads to enhanced processing of social stimuli, by increased in-group trust, increased emotion recognition, and increased eye contact.[4] Oxytocin has been shown to increase activity in brain structures involved in processing socially meaningful stimuli.[5] Oxytocin also has numerous brain targets, including but not limited to the amygdala, hippocampus, hypothalamus, and nucleus accumbens. Therefore, it may be postulated that treatment with oxytocin would normalize social behaviors and memory, while decreasing anxiety and parasympathetic activation (fear/stress).[3]

Oxytocin treatment has recently also been considered in autism for reasons other than its social effects.[1,2] Namely, the oxytocin gene has shown aberrations in genetic association studies of ASD;[6–9] ; a reduction of oxytocin mRNA has been shown in the temporal cortices of individuals with ASD;[7] variation in the oxytocin receptor (*OXTR*) gene differentially effects the neuroendophenotype of youth with ASD;[10] and, abnormal oxytocin blood levels have also been measured in individuals with ASD.[11–13] All of these instances point to the potential for oxytocin to improve aspects of ASD.

A number of existing studies have investigated the effects of oxytocin in autism and related animal models. In mice, knockout of the oxytocin receptor caused a resistance to change and social deficits (behaviors characteristic of autism), which was normalized after acute treatment with oxytocin.[14] Subchronic oxytocin administration in strains of mice with social deficits or repetitive behaviors increased sociability in both strains.[15] Social behavior in a genetic mouse model of autism was restored by oxytocin treatment.[16] Multiple studies have shown an increase in emotion recognition abilities and increased ability to process socially relevant cues in animal models of autism administered a single dose of oxytocin.[17] A relatively small study (n=19) of chronic administration of oxytocin in individuals with autism found improvements in measures of social cognition and quality of life.[1]

However, there are several shortcomings in our current understanding of oxytocin as a potential pharmacological treatment for ASD. First, although there is an extensive wealth of literature on the acute effects of oxytocin, few studies have investigated the chronic effects. Given the lifelong nature of the disorder and its symptoms, chronic treatment is likely the only way amelioration of autism symptoms would occur.

Moreover, there is a gap in our knowledge surrounding oxytocin's effects on the brain. Some studies have shown that oxytocin attenuates amygdala response to faces, regardless of valence.[5] Other studies found, using functional magnetic resonance imaging (fMRI) that oxytocin enhanced brain function (multiple regions) in children with ASD.[4] As mentioned before, oxytocin receptor locations are known,[3] but our understanding of where the drug goes after administration is limited.

This problem is further exacerbated by the pharmacology of oxytocin. The neuropeptide is too large to cross the blood brain barrier and has a very short half-life.[18] Therefore, an administration method is needed that quickly and directly allows oxytocin to enter the brain. Though methods like intracerebroventricular (ICV) infusion and peripheral injections have been used in animal models, there is a need for a method that is easily employed by humans (as opposed to the intravenous (IV) lines used for labour induction). Intranasal administration allows for simple, non-invasive treatment that circumvents the issues with the blood brain barrier and is easily used both in humans and in mice.[18]

Importantly, given the substantial heterogeneity of ASD, there is a need for studies to delineate phenotype-based subsets that may respond to oxytocin treatment.[19] This is perhaps best demonstrated by Engelman and colleagues (2008) in their co-clinical study of lung cancer.[20] A clinical trial of a promising therapeutic failed to show treatment effect in their population. They simultaneously treated three different genetic knockout mouse strains, with the same treatment used in humans. The group realized that two of the strains responded 100% to the treatment, while one did not. Armed with this genetic information, they divided the clinical population into subsets by genotype and found that, in fact, all the patients not carrying the genetic mutation of the non-responder mouse model improved with the treatment. To this end, a study is necessary that incorporates numerous phenotypes across multiple mouse lines, and also makes use of multivariate analyses to inform clinical trials, all in the context of ASD.

Numerous studies have spoken to the utility of magnetic resonance imaging (MRI) in the stratification of ASD individuals into biologically homogeneous subgroups.[19,21–24] Magnetic resonance imaging (MRI) offers the ability to quantify the structural phenotype of both mice and humans, allowing for whole brain coverage and translatability to human imaging studies, both in acquisition and analysis.[23,25–28] It also affords the additional advantages of high-throughput, having a link with behavior,[25,29–31] showing evidence of plasticity with exposure,[32,33] and having sensitivity to the neurological effects of interventions like drugs.[32–41]

To explore if we could understand patterns of response in mice, we executed a mouse study in parallel, akin to a co-clinical trial. Specifically, a large randomized, double-blind, placebo-controlled, preclinical study on chronic intranasal oxytocin treatment in three different mouse models related to autism was performed. A wide range of behavioral and neuroanatomical phenotypes were assessed, in a high-throughput method of treatment evaluation.

2 Methods

2.1 Subjects

Three in-bred strains of autism mouse models were used: the *16p11.2* heterozygous knockout (B6129S-Del(7Slx1b-Sept1)4Aam/J; JAX #013128)[42](henceforth referred to as "*16p*"), the *Fmr1* hemizygous knockout (FVB.129P2-Pde6b+ Tyrc-ch Fmr1tm1Cgr/J; JAX #004624)[43](henceforth referred to as "*Fmr1*"), and the *Shank3* exon 4-9 (ANK domain) homozygous knockout (B6(Cg)-Shank3tm1.2Bux/J; JAX #017890)[44](henceforth referred to as "*Shank3*"). The mice were on the following background strains, respectively: B6129SF1/J (JAX #101043)(henceforth

referred to as "129"), FVB.129P2-Pde6b+ Tyrc-ch/AntJ (JAX #004828)(henceforth referred to as "FVB"), C57BL/6J (JAX #000664)(henceforth referred to as "C57").

(a) Totals- Behavior

Strain	Total	Oxytocin	Placebo
16p	30	15	15
129	29	15	14
Fmr1	29	14	15
FVB	30	13	16
Shank3	36	17	19
C57	26	12	14

(b) Totals- Sociability

Strain	Total	Oxytocin	Placebo
16p	14	9	5
129	17	10	7
Fmr1	18	8	10
FVB	18	10	8
Shank3	29	13	16
C57	19	10	9

Table 1: Tables depicting the sample size in each strain, broken down by treatment. A minimum of n=14 was aimed for per genotype, per strain, per treatment. Table (a) shows the samples for all behaviors except sociability. Table (b) shows the reduced sample size due to failed acquisition in the sociability tri-chamber test.

Totals- Imaging

Timepoint	5wks		8wks		9wks		*Ex vivo*	
Strain	Oxy	Pl	Oxy	Pl	Oxy	Pl	Oxy	Pl
16p	6	6	6	9	10	10	15	15
129	3	9	7	8	9	12	14	15
Fmr1	10	8	11	9	11	7	15	14
FVB	14	14	14	12	12	10	16	13
Shank3	19	16	19	16	18	12	19	17
C57	13	11	14	12	12	12	14	12

Table 2: Table depicting the number of images that passed quality control at each imaging time point in each strain, broken down by treatment. A minimum of n=14 was aimed for per genotype, per strain, per treatment. Although all mice were scanned at all time points, some images were excluded due to motion artifacts or low SNR.

Active colonies for each strain were maintained at The Center for Phenogenomics (TCP). Breeders were set up to yield control litter-mates for each strain. Mice were group housed, and an attempt was made to achieve a sample size of 14 male mice per genotype, per strain, per treatment (Table 1). Data was collected and analyzed for all mice for all behavioral tests, except for sociability. Technical issues lead to the loss of approximately 40% of the social behavior data, reduced sample sizes are displayed in Table 1b.

All studies and procedures were approved by the TCP Animal Care Committee, in accordance with recommendations of the Canadian Council on Animal Care, the requirements under the Animals for Research Act, RSO1980, and the TCP Committee Policies and Guidelines. Mice were maintained under controlled conditions (25 C, 12 hour cycle) at TCP in sterile, individually ventilated cages and were provided standard chow (Harlan, Teklad Global) and sterile water *ad libitum* via an automated watering system.

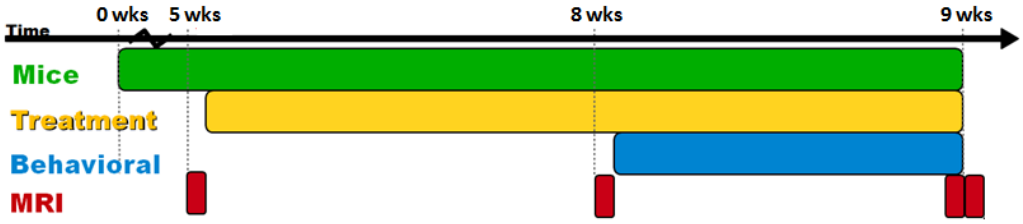

Figure 1: Time-line illustrating the project design. Green indicates the life of the mice, yellow indicates treatment administration, blue indicates period of behavioral testing, while red indicates occurrences of magnetic resonance imaging (MRI).

2.2 Experimental Time-line

The experimental time-line is outlined in Figure 1. At five weeks of age, mice underwent *in vivo* manganese-enhanced magentic resonance imaging (MEMRI) scanning and were randomly assigned to a treatment group (oxytocin or placebo) such that the experimenter remained blinded. Mice were treated everyday, for 28 days total. After an *in vivo* MEMRI scan at postnatal week 8, mice were assessed on four different behavioral paradigms, while still receiving treatment. At nine weeks of age, the mice were scanned with *in vivo* MEMRI once more, perfused, and scanned *ex vivo* at a later time-point. The study was designed to be an exploratory study and therefore no primary outcome was defined before the study started.

2.3 Oxytocin Treatment

Oxytocin (Sigma-Aldrich) was dissolved in saline and administered intranasally everyday for 28 days. Each morning, between 10am and 11am, the mice received a volume of 10ul, a dose of 0.6 IU. This dose was chosen to be 0.6IU, too low to produce peripheral effects and similar to the quantity used in humans.[45] Control mice received the same quantity of saline (placebo). A similar protocol was used as Huang et al (2014):[17] a 200-ul Eppendorf pipette was used for administration, and drops of the solution were gently placed equally on both nostrils of each mouse. The primary experimenter was blinded to treatment and genotype, and was only unblinded at the time of analysis, when experiments were over.

2.4 Behavioral Phenotype

On the third week of treatment, the mice were assessed for repetitive behaviors (as assessed by grooming), social behaviors (three chamber sociability task), anxiety and hyperactivity (open field), learning and motor coordination (rotarod), and memory (novel object recognition).

2.4.1 Statistics

Behavioral data was analyzed using the R statistical language (R Core Team, 2016).[46] The data was assessed in two ways, to look at a general treatment effect across genotypes and background strains, as well as within strain.

In the former, a linear mixed effects model was used, because they incorporate both fixed and random effects and are useful for longitudinal data, as well as un-

balanced study designs[47,48] (see Vousden et al 2018[49] and Qiu et al 2018[50] for fuller explanations on similar data). In this case, linear mixed effects models were created and compared using log-likelihood tests to determine the effect of genotype (defined as wildtype, *16p*, *Fmr1*, or *Shank3*) and treatment, and their interaction on each behavioral test (see Equation 1). Random intercepts for each background strain were incorporated.

$$\begin{aligned} y_{ij} = \beta_0 + \beta_1 Genotype + \beta_2 Treatment + \beta_3 Genotype{:}Treatment + b_i Strain_i + \epsilon_{ij} \\ \text{where } Genotype \text{ is defined as wildtype, } \textit{16p}\text{, } \textit{Fmr1}\text{, or } \textit{Shank3}\text{,} \\ \text{and } Strain \text{ is defined as 129, FVB, or C57,} \\ \text{and } y_{ij} \text{ is the } j^{th} \text{ measurement of the dependent variable for strain } i. \end{aligned} \tag{1}$$

Additional information regarding treatment response and genotype effect was assessed by subsetting by background strain (129, FVB, C57) and using traditional linear regression analysis (see Equation 2). For each strain, separate linear models were created and compared using ANOVA, to determine whether a particular fixed effect (treatment, genotype, or their interaction) significantly improved the model. The distribution within strain of each behavioral test was also assessed and corrected for, before analysis. The genotype effect was used to compare to existing behavioral literature. All data was corrected for multiple comparisons using false discovery rate (FDR) correction,[51] with p-values pooled by treatment, genotype, and interaction independently.

$$\begin{aligned} y_i = \beta_0 + \beta_1 Genotype + \beta_2 Treatment + \beta_3 Genotype{:}Treatment + \epsilon_i \\ \text{where } Genotype \text{ is defined as wildtype or mutant,} \\ \text{and one model was created for each of the background strains,} \\ \text{and } y_i \text{ is the measurement of the dependent variable for mouse } i. \end{aligned} \tag{2}$$

To explore the multivariate nature of the project, principle component analysis (PCA) was employed. Due to the reduced sample size in the sociability data, analyses were done on two sets of the data: 1) all mice that had grooming, open field, and rotarod data ("all mice, no sociability data")(see Table 1a), and 2) the subset of mice that had grooming, open field, rotarod, and sociability data ("subset of mice that have sociability data")(see Table 1b).

2.4.2 Behavioral Tests

A description of each of the behavioral tests follows,[52,53] in the order they were performed:

Sociability The three-chambered sociability apparatus consists of a rectangular box with three chambers, with a wire cup placed in either side chamber. The mouse is habituated for 10 minutes during which it can access all three chambers. After this time, a novel stranger mouse is placed under a wire-cup in one of the side chambers. The mouse is observed for an additional 10 minutes during which measures such as time (s) spent in each of the three chambers, specifically near/sniffing the wire cups (near the novel mouse) are observed using an overhead video system,

manually scored, and then compared. Mice that are not considered social spend either an equivalent amount of time between the two cups or show a preference for the empty cup (away from the novel mouse).

Rotarod The rotarod test was run on a system (Rota-rod/RS, Panlab, Harvard Apparatus) with the capacity to run up to five mice at a time (though no more than three were ever run). For the rotarod test, mice go through two types of trials, pre-trials and test-trials, over two days. Pre-trials are sessions where the mice are allowed to learn how to stay on the rod for 10s, when it is only rotating at 4 revolutions per minute (rpm). The number of attempts it takes before the mouse stays on the rod for the entire duration is recorded. Latency to fall off the rod is the primary measure of the rotarod test. The mice are given three trials of a total possible five minutes for each trial. The rod starts off at 4rpm and slowly accelerates over the course of 5 minutes. The latency (s) to fall off the rod is recorded, averaged, and compared. Mice that either have a learning and memory deficit or a motor deficit, perform worse on one or both measures when compared to wildtype controls.

Grooming For the grooming test, the mice are placed into an empty standard cage (Green Line IVC Sealsafe PLUS Mouse, Techniplast) for ten minutes (habituation). The following ten minutes, mice are placed into a different, empty, standard cage and observed for grooming behaviors. Primary measures are duration of grooming bouts (s) as well as number of grooming bouts. Mice with a repetitive behavior phenotype spend significantly more time grooming, with more bouts of grooming, than wildtype controls.

Open Field The open field test consists of 10 minutes of testing, where the mouse is placed in an empty box (area=44cm^2) and allowed to roam free for the duration of the test. The mouse's motion is recorded by a system (Activity Monitor 7, Med Associates Inc, Fairfax VT) and primary measures investigated are time (s) spent in the center (decreased anxiety) and total distance (cm) moved (hyperactivity).

It should be noted that mice underwent a fifth behavioral test during the study (after the other behavioral tests), the novel object recognition test. This data was removed from the analysis in it's entirety once it was discovered that the tracking software was not accurately capturing the mouse's behavior.

2.5 Neuroanatomical Phenotype

Mice were injected in their intraperitoneal (I.P.) cavity with a manganese (Mn) contrast agent up to 24 hours before the scan. A multi-channel 7.0T magnet (Agilent Technologies) was used that allows up to 7 animals to be scanned simultaneously. The mice were anesthetized using 1% isoflourane during T1-weighted scanning with 90 um isotropic resolution (TR=29ms, TE=5.37ms, 1 hour 52 minute scan time). The animals' breathing and temperature were monitored. Mice were imaged at 5, 8, and 9 weeks of age.

One *ex vivo* MRI scan was performed at least a month after the mice were sacrificed.[54] The procedure followed closely follows the procedure described in Lerch

et al 2011[25] and Nieman et al 2018.[28] To prepare the brains for scanning and enhance contrast, a fixation and perfusion procedure was done as previously described in Cahill et al 2012.[55] The same multi-channel 7.0T magnet (Varian Inc, Palo Alto, CA) was used, with the ability to scan up to 16 brains simultaneously. A T2-weighted 3D fast spin echo sequence was used to yield an isotropic resolution of 40 um (cylindrical acquisition, TR=350ms, TE=12ms, 14 hour scan time).[56]

Data from both imaging types was analyzed using image registration and deformation based morphometry approaches as described in Lerch et al (2011).[25] Briefly, images were linearly (6 parameter, then 12 parameter) and nonlinearly registered together. At completion of this registration, all scans were deformed into alignment with each other in an unbiased fashion. These registrations were performed with a combination of MNI autoreg tools[57] and ANTS (advanced normalization tools).[58,59] The changes within regions and across the brain can be examined using deformation based morphometry (DBM) and MAGeT (a multi-atlas registration-based segmentation tool).[60] An atlas that segments 159 structures in the adult mouse brain was used for the *in vivo* image analysis, and the *ex vivo* analysis has further delineations resulting in a total of 182 distinct regions.[50,61–64] Segmentations of all brains passed quality control by visual inspection (see Table 2).

2.5.1 Statistics

Data from both imaging methods was analyzed using the R statistical language (R Core Team, 2016)[46] using linear mixed effects models (Lmer).[47,48] As with the behavioral data, linear mixed effects models were used to determine the effect of genotype (defined as wildtype, *16p*, *Fmr1*, or *Shank3*) and treatment on the volume for each region of interest (ROI) or voxel (Equation 3). Random intercepts for each background strain were incorporated. A log-likelihood test was performed to assess the significance of treatment and genotype, and their interaction. Data was analyzed as absolute volumes as well as relative volumes by covarying for total brain volume.[65]

To assess the effect of treatment on time, brain region volume at the 5 weeks *in vivo* scan point was used to predict, along with genotype and treatment, the latter brain region volumes (Equation 4). For simplicity, relative volumes were calculated as proportion of total brain volume. Additional information about the genotype effects was also analyzed by subsetting by background strain and assessing the main effects of genotype (mutant versus wildtype) and treatment using linear models in the *ex vivo* dataset (Equation 5). Multiple comparisons in the data from all analyses was corrected for using false discovery rate (FDR) correction,[51] with p-values pooled by treatment, genotype, and interaction independently.

$$y_{ij} = \beta_0 + \beta_1 Genotype + \beta_2 Treatment + \beta_3 Genotype{:}Treatment + b_i Strain_i + \epsilon_{ij}$$
$$\text{where } Genotype \text{ is defined as wildtype, } 16p, Fmr1, \text{ or } Shank3,$$
$$\text{and } Strain \text{ is defined as 129, FVB, or C57,} \quad (3)$$
$$\text{and } y_{ij} \text{ is the } j^{th} \text{ measurement of the dependent variable for strain } i.$$

$$LaterVolume_{ij} = \beta_0 + \beta_1 EarlyVolume + \beta_2 Genotype + \beta_3 Treatment + \beta_4 Genotype{:}Treatment + b_i Strain_i + \epsilon_{ij}$$
where *Genotype* is defined as wildtype, *16p*, *Fmr1*, or *Shank3*, and *Strain* is defined as 129, FVB, or C57, and y_{ij} is the j^{th} measurement of the dependent variable for strain i. (4)

$$y_i = \beta_0 + \beta_1 Genotype + \beta_2 Treatment + \beta_3 Genotype{:}Treatment + \epsilon_i$$
where *Genotype* is defined as wildtype or mutant and one model was created for each of the background strains, and y_i is the measurement of the dependent variable for mouse i. (5)

3 Results

3.1 Chronic intranasal oxytocin treatment has little to no effect on the behavioral phenotype of autism-related mouse models

No significant effect of oxytocin treatment was found on social behavior, regardless of strain or genotype when analyzing the sample as a whole (Figure 2A and E). A significant effect of treatment was found when subsetting for the FVB background strain, with treatment normalizing a deficit in the number of bouts of grooming in the *Fmr1* mouse model (q=0.012)(Figure 2B). No other effects survived correction for multiple comparisons (see Figure 3A).

Without correction for multiple comparisons, when subsetting for background strain, some trends for treatment were observed. Treatment appeared to decrease the amount of time spent in the center of the open field in the *16p* (p=0.048) and the *Fmr1* (p=0.086, non-significant interaction) mice (Figure 2F). Treatment also had an interesting trending effect on the C57 mice (*Shank3* control), by decreasing performance on the rotarod pretrials (interaction p=0.070)(Figure 2C) and increasing hyperactivity in the open field (interaction p=0.093), while not having an effect on the *Shank3* mutant mice (Figure 2D).

PCA was employed to further elucidate if a treatment effect was present that was not captured in the individual behaviors but would be captured given a multivariate analysis. Two analyses were run on separate subsets, the first on the full data-set excluding social behaviors ("all mice, no sociability data")(see Table 1a), and the second on the subset of mice that had social behaviors tested ("subset of mice that have sociability data")(see Table 1b). The first two components accounted for 52.5% and 48.2% of the total variance, respectively, of the two datasets (see Figure 3C,D). Most of the behavioral tests exhibited negative values for principle component 1 (PC1), in both sets. In contrast, the pre-trials measure of rotarod and the average duration of grooming bouts were positive in both sets. No distinct groups of variables were distinguishable, although measures from the same behavioral test did coincide. Overall, no pattern of treatment response was observed.

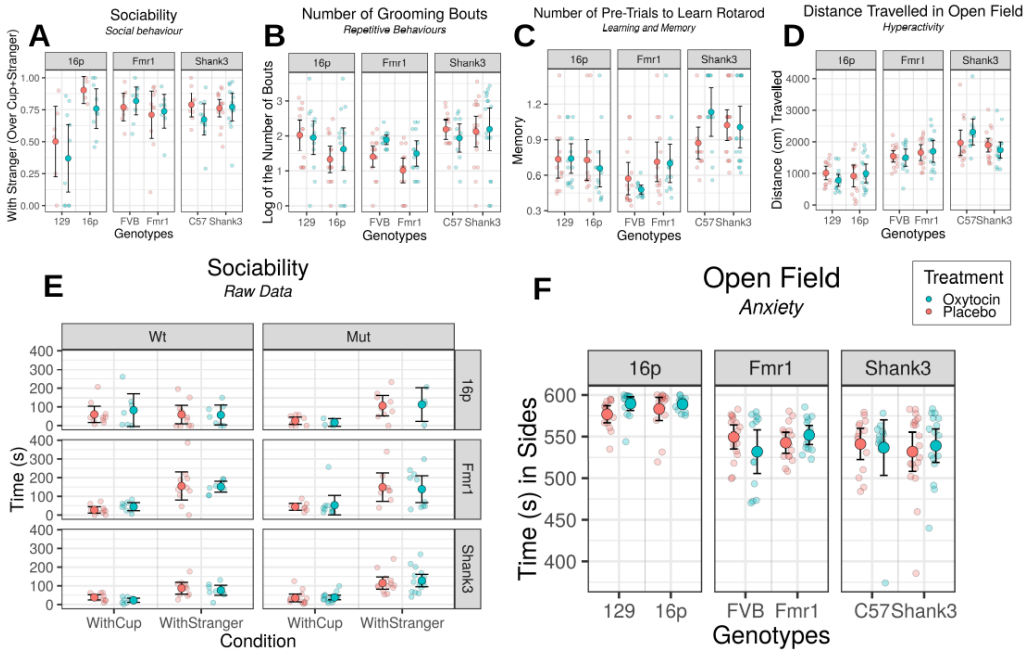

Figure 2: Figures depicting treatment effect in each strain, by genotype. Blue indicates mice treated with oxytocin, red indicates mice treated with saline (placebo). Each point represents one mouse. Bars show mean ± confidence interval (95%). Sociability data is shown both as (**E**) the raw time spent with the mouse and cup, for each mouse by genotype and strain, as well as (**A**) a ratio of time with stranger over total time with cup and stranger. (**B**) Number of bouts of grooming in the mice, (**C**) number of pre-trials required to learn rotarod, (**D**) distance travelled in the open field, and (**F**) time spent in the sides ($= total - center$) of the open field are also shown.

3.2 Chronic intranasal oxytocin treatment has a trending effect on the neuroanatomy of autism-related mouse models

Chronic treatment with oxytocin had a weak and focused effect, only changing the volume of the cerebellar peduncle superior and the endopiriform claustrum (intermediate nucleus) regions when assessing relative volumes (see Figure 5), across all mouselines (using Equation 4). No other brain regions were significant with correction for multiple comparisons, but the pattern of treatment effect, as shown by the voxel-wise analysis, shows alterations in several cerebellar regions, the cingulate cortex, and, interestingly, several regions related to sensory/motor behaviors, like the cuneate nucleus, the dorsal tenia tecta, and the superior olivary complex.

The *ex vivo* analysis (using Equation 3), showed no significant treatment effect (see Figure 7), only a weak trend (FDR = 0.195) in the *Shank3* interaction of cerebellar lobule 9 (white matter). When assessing strain differences (using Equation 5), the *Shank3* mice showed trending (FDR = 0.161) treatment effect in three regions of the primary somatosensory cortex and the lateral ventricles. As seen in Figure 7, the genotype differences were significant and widespread, though more so for the *16p* and *Fmr1* mice.

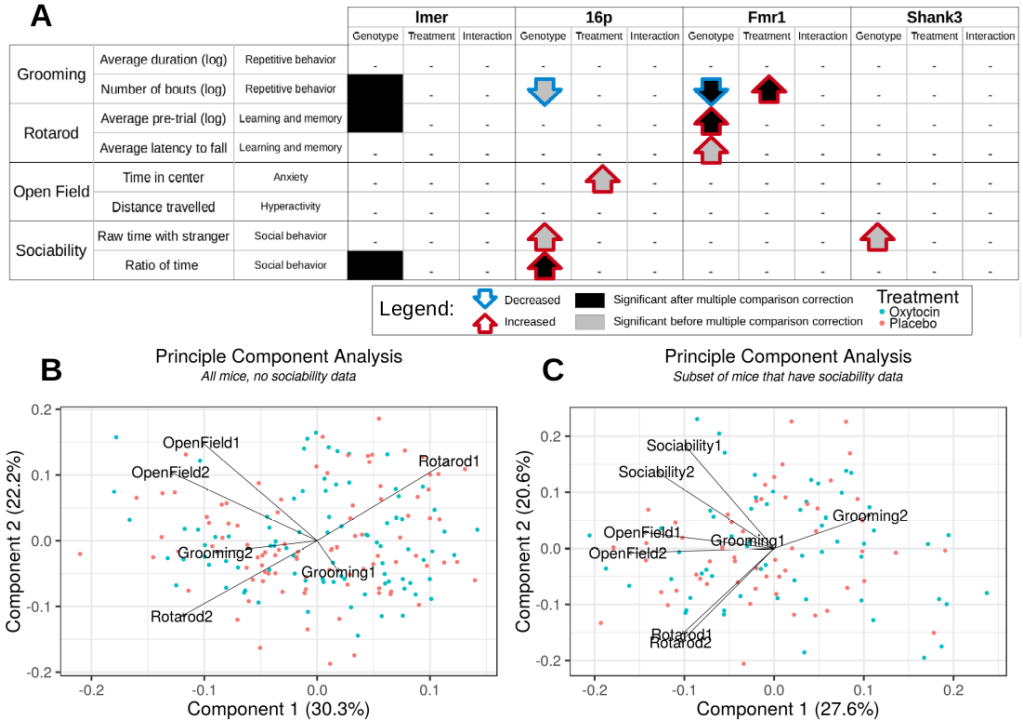

Figure 3: Table **A** shows the results of the log-likelihood tests assessing the main effects of treatment and genotype, and their interaction from the linear mixed effects models on the behavioral tests. Each of the behavioral tests are shown, broken down by measure. The table is color-coded to show significant, correct FDR values (<0.05) with a dark background, and trending (<0.10) values with a grey background. Figures **B** and **C** show the results of the PCA analyses, with the "all mice, no sociability data" set on the left (**B**) and the "subset of mice that have sociability data" on the right (**C**). The names of the PCA measures follow down along the table of measures. Specifically, Grooming1 is "average duration" (the first row in the table), Grooming2 is "number of bouts" (second row), Rotarod1 is "average pre-trials" (3rd row), Rotarod2 is "average latency to fall" (4th), OpenField1 is "time in center" (5th), OpenField2 is "distance travelled" (6th), Sociability1 is "raw time with stranger" (7th), and Sociability2 is "ratio of time" (last row). As evident from these tables and figures, little to no treatment effect was observed across the multitude of behavioral phenotypic measures employed in this study.

4 Discussion and Conclusions

Chronic treatment with intranasal oxytocin produced subtle behavioural and neuroanatomical effects across three different autism mouse models. No significant effect of treatment was found on social behavior, although a significant effect of treatment was found in the *Fmr1* mouse, with treatment normalizing a grooming deficit. No other treatment effect on behavior was observed that survived multiple comparisons correction. No pattern of treatment effect was distinguishable when a multivariate method (PCA) was employed. Treatment effect on the neuroanatomy was modest, and primarily apparent when assessing relative volumes.

Although not statistically significant, the pattern of treatment effect in the brain is particularly promising because many are regions that are associated with oxytocin signaling and, moreover, have been implicated in autism pathogenesis. For example, the brain stem and olfactory systems have large populations of oxytocin receptors,

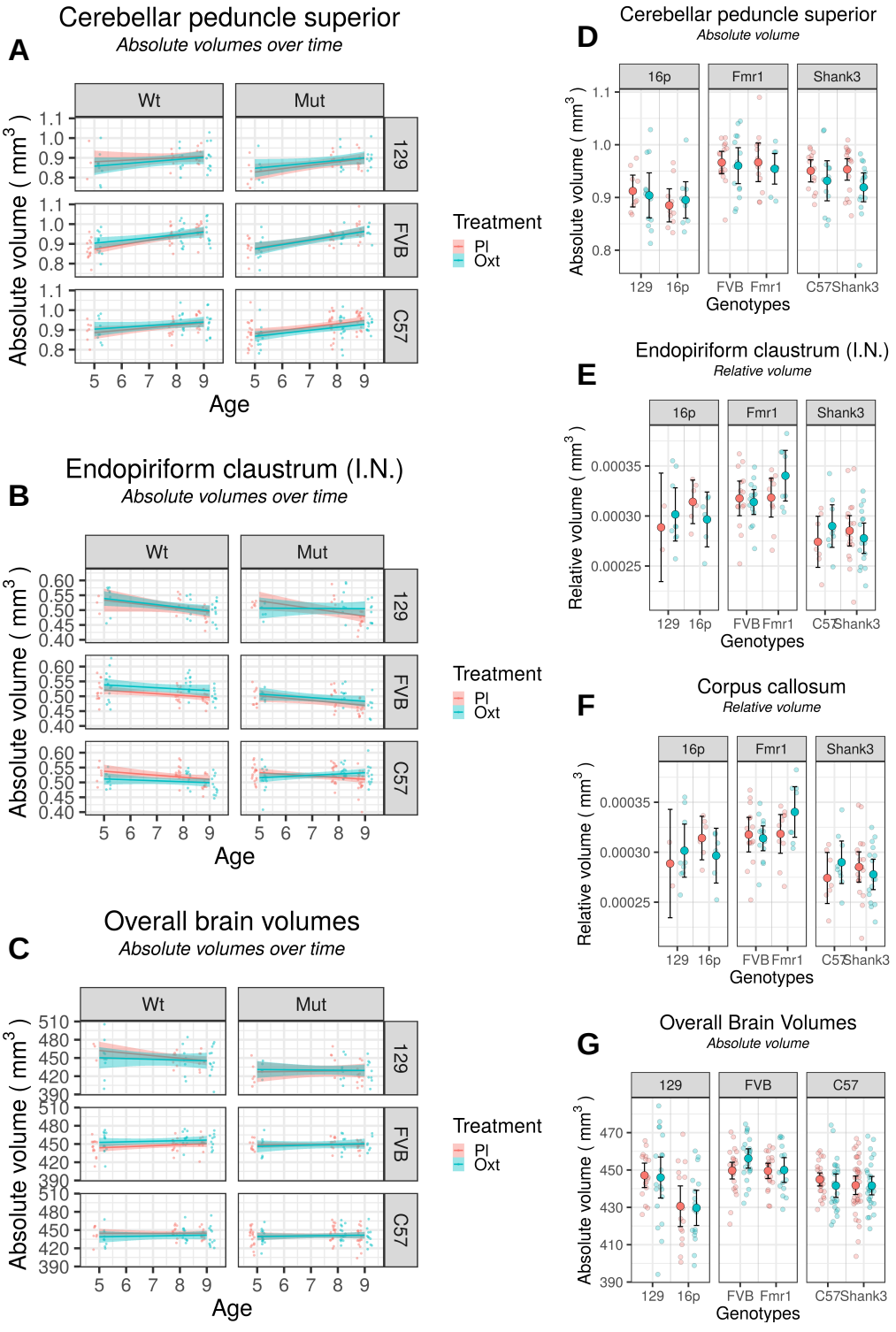

Figure 4: Figures depicting treatment effects of selected regions from *in vivo* imaging. Figures **A** through **C** show the change in volume over time of the cerebellar peduncle superior, the endopiriform claustrum, and the total brain volumes. Figures **D** through **G** show a cross-sectional view of the brain region volumes after 3-4 weeks of treatment, faceted by strain. To better see the treatment effect, two of the figures (**E** and **F**) show relative volume of the regions. With correction for multiple comparisons, no significant treatment effect was seen on any region, though the cerebellar peduncle superior and endopiriform claustrum (intermediate nucleus) showed trending (FDR=0.155) effects (see 5). There were significant genotype differences across brain regions, and overall brain volume.

and we found (trending) treatment effects in the cuneate nucleus, the superior olivary complex, and the dorsal tenia tecta, among other regions. The superior cerebellar peduncle– a region found to have a trending treatment effect– is a white matter tract that connects the cerebellum to the midbrain. A number of studies have shown aberrations in the structure and function (See Crippa et al 2016[66] for review, also Cheng et al 2010[67]) of the superior cerebellar peduncle in autism. Moreover, the cerebellum, as a whole, has been implicated in the ethiopathogenesis of autism (for review, see Fatemi et al 2012,[68] Crippa et al 2016[66]). An elegant study in a mouse model of autism demonstrated the important role of the cerebellum in autism-related behaviors, including the therapeutic potential of cerebellar neuromodulation in autism.[69] The endopiriform claustrum, another region that was found to have a trending treatment effect, is a part of the basal ganglia, the system known to regulate repetitive behaviors. Although the exact function of the claustrum is unknown, it is hypothesized that it plays a role in multisensory integration and is an important relay nucleus to the cortex.[70] Furthermore, a number of regions in the Shank3 mouse model found to be affected by treatment, are related to sensation/perception. There is a wealth of literature on the dysfunction of sensation/perception in autism (see Robertson and Baron-Cohen (2017)[71] for review). Overall, oxytocin's effects on these regions– although modest– are promising for the treatment of autism.

To compare to existing literature, the effect of genotype of the three mutant mice was separately analyzed (see Equations 2 and 5). Without correction for multiple comparisons, all three mutant mice, for the most part, showed behavioral and neuroanatomical differences that were expected based off previous literature. With multiple comparison correction, this study moderately recapitulated existing literature.

There are many possible reasons this study did not see a significant effect of treatment on behavior. Although many studies have investigated the promising effects of oxytocin in autism and related models, the majority of those studies investigated the acute effects of treatment. One study in rodents found opposing results for acute vs chronic oxytocin administration,[17] while another specifically focusing on the social effects of oxytocin, found that chronic administration actually hinders some social behaviors in prairie voles.[45] Furthermore, a study of chronic oxytocin treatment in autism patients only found improvements on one secondary measure.[1] As Huang et al (2014) put it, there seems to be a "translational hurdle" in the movement of oxytocin from acute studies to chronic.[17]

Another possible issue for the lack of treatment effect may be due to the study population. We chose to limit the study to older (adolescent/adult) mice to minimize variability and increase our power. However, it is possible that a younger population is needed to see the effects of oxytocin. For example, the association of the plasma oxytocin levels in autism (that was mentioned earlier as a promising reason we expect response to oxytocin) was found in children, and perhaps does not extend to adults.[13] Developmental processes occur during childhood that could impact the effect of treatment response.[72–74]

Moreover, some limitations arose during this study. For example, the time-line was designed to maximize high-throughput and therefore some potentially insightful behavioral tests were omitted. Given the number of brain regions involved in sensation/perception that showed changes due to treatment, a test that specifically

A

	In vivo					
	Absolute			Relative		
	Treatment	Genotype	Interaction	Treatment	Genotype	Interaction
Cerebellar peduncle superior	0.743	0.945	0.999	0.155	0.935	0.970
Endopiriform claustrum (I.N.)	0.743	0.029	0.999	0.155	0.001	0.919

B

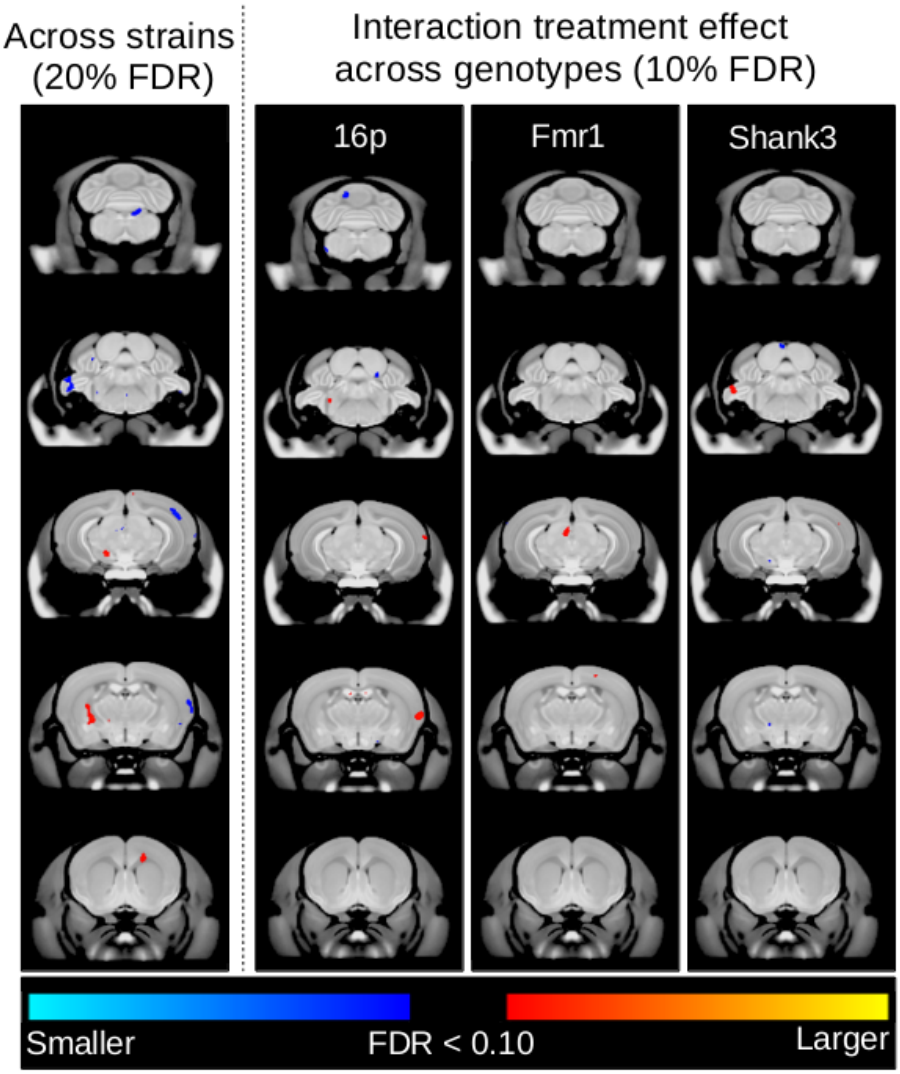

Figure 5

Figure 6: Treatment effect in the *in vivo* data. Top (**a**) shows the results of the volume-wise linear mixed effects model with main effects of treatment and genotype, with a random intercept for each background strain (using Equation 4). FDR-corrected values are shown with black background indicating significance (<10%) and grey background showing trends. Results from both absolute and relative volume analyses are shown; in this case, relative volumes of each region were calculated as proportion of the total brain volume. The cerebellar peduncle superior and the endopiriform claustrum (I.N. = intermediate nucleus) showed subtle treatment effects. Bottom (**b**) shows the voxel-wise data analysis, using the linear mixed effects model shown in Equation 3.Colors indicate voxels that were at least 10% FDR significant, with red indicating regions that were larger than the reference group and blue indicating smaller. In the case of the treatment effect across strains (left), colours indicate FDR 20%, to better distinguish patterns. These figures clearly depict the subtle effect of treatment response on neuroanatomy.

evaluated those behaviors may have seen a significant effect of treatment. The reduced sample size (Table 1) for the sociability test (due to failed acquisition) could have also contributed to the lack of treatment effect, due to low power.

Furthermore, there is no current robust method to assess the quantity of oxytocin that is delivered to the brain using the intranasal method. When the treatment was first started, all the mice fought the scruff hold and intranasal administration equally. Near the end of the treatment period, however, approximately half the mice would fight the treatment while the other half remained stationary. The authors assume the mice that ceased avoiding the intranasal application were the ones to receive oxytocin and, through classical conditioning, had learned that the application would quickly lead to pleasant sensations.[3] Though this was primarily observational, a small sample of mice (n=14) were assessed to see if treatment arm (placebo vs. oxytocin) could be determined just through interaction during treatment after 3 weeks of treatment. With the help of a colleague, the correct treatment arm was confirmed for all the mice in the sample. Although not specific to the brain, this confirms that the intranasal application method was successful in administering oxytocin into the mice.

It remains possible that the treatment effects that were observed were solely due to peripheral treatment effects. Gareth Leng and Mike Ludwig (2016)[75] argue that it is unlikely that any intranasal method has successfully delivered oxytocin to the brain and the effects that are seen, for example in Neumann et al 2013,[18] are due to the oxytocin signaling system responding to peripheral changes in oxytocin levels. More tests that assess the utility of intranasal oxytocin, like proper dose-response studies, with peripheral effects controlled for,[75] are necessary.

Future studies should aim to explore other behavioral tests, population sets, and administration methods. The possibility remains that the three autism mouse models employed in this study– the *16p*, *Fmr1*, and *Shank3* mouse models– are non-responders to oxytocin. Despite the limitations, the study is one of very few studies to assess the effects of chronic oxytocin treatment on mouse models of autism. It also established a rigorous method of assessing treatment effect in preclinical models, on both behavioral and neuroanatomical metrics, to help inform future clinical trials.

5 Acknowledgements

This work was supported by funding from the Brain Canada Foundation, The Azrieli Foundation, Health Canada, Province of Ontario Neurodevelopmental Disorders (POND) Network, and the Ontario Brain Institute (OBI). Z.L. was supported by the developmental neurosciences research training award from the Brain Canada Foundation, Kids Brain Health Network, and the Hospital for Sick Children.

The authors would additionally like to thank Darren Fernandes, Chris Hammill, Dr. Dulcie Vousden, and Matthijs Van Eede for helping with data analysis, Christine Lalilberte, Dr. Dulcie Vousden, and Dr. Jill Silverman for procedural assistance, and Drs. Brad Wouters and Mark Henkelman for advice and guidance.

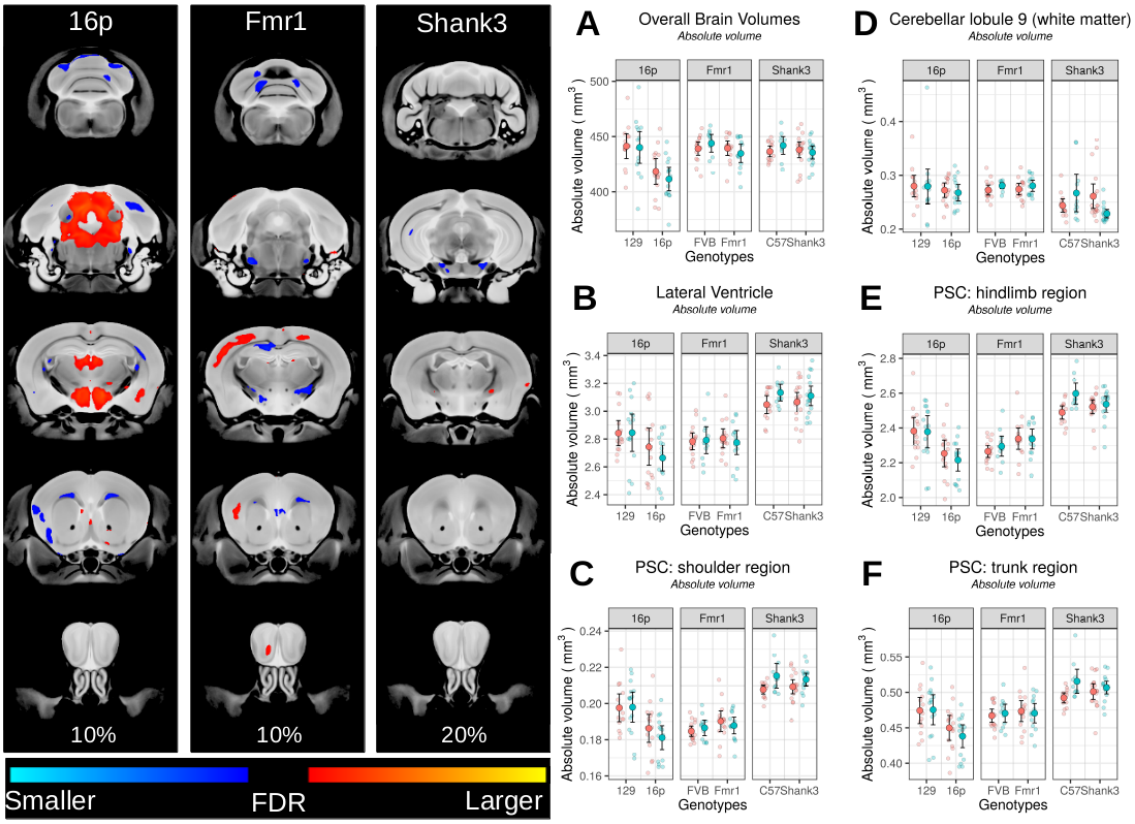

Figure 7: Figures depicting the results of the *ex vivo* analyses. On the left, genotype effects are shown from the subsetted (by background strain) voxel-wise analyses (Equation 5). On the right, the graphs depict treatment effect across strains for six regions, including overall brain volumes. PSC= Primary Somatosensory Cortex

References

[1] Evdokia Anagnostou, Latha Soorya, William Chaplin, Jennifer Bartz, Danielle Halpern, Stacey Wasserman, A. Ting Wang, Lauren Pepa, Nadia Tanel, Azadeh Kushki, and others. Intranasal oxytocin versus placebo in the treatment of adults with autism spectrum disorders: a randomized controlled trial. *Mol Autism*, 3(1):16, 2012.

[2] Luis de la Torre-Ubieta, Hyejung Won, Jason L Stein, and Daniel H Geschwind. Advancing the understanding of autism disease mechanisms through genetics. *Nature Medicine*, 22(4):345–361, 4 2016.

[3] E. E. Benarroch. Oxytocin and vasopressin: Social neuropeptides with complex neuromodulatory functions. *Neurology*, 80(16):1521–1528, 4 2013.

[4] I. Gordon, B. C. Vander Wyk, R. H. Bennett, C. Cordeaux, M. V. Lucas, J. A. Eilbott, O. Zagoory-Sharon, J. F. Leckman, R. Feldman, and K. A. Pelphrey. Oxytocin enhances brain function in children with autism. *Proceedings of the National Academy of Sciences*, 110(52):20953–20958, 2013.

[5] Gregor Domes, Markus Heinrichs, Ekkehardt Kumbier, Annette Grossmann, Karl-heinz Hauenstein, and Sabine C Herpertz. Effects of Intranasal Oxytocin on the

Neural Basis of Face Processing in Autism Spectrum Disorder. *Biological Psychiatry*, pages 1–8, 2013.

[6] Douglas C Bittel, Nataliya Kibiryeva, Majed Dasouki, Joan H.M. Knoll, and Merlin G Butler. A 9-year-old male with a duplication of chromosome 3p25.3p26.2: Clinical report and gene expression analysis. *American Journal of Medical Genetics Part A*, 140A(6):573–579, 3 2006.

[7] Simon G Gregory, Jessica J Connelly, Aaron J Towers, Jessica Johnson, Dhani Biscocho, Christina A Markunas, Carla Lintas, Ruth K Abramson, Harry H Wright, Peter Ellis, Cordelia F Langford, Gordon Worley, G Robert Delong, Susan K Murphy, Michael L Cuccaro, Antonello Persico, and Margaret A Pericak-Vance. Genomic and epigenetic evidence for oxytocin receptor deficiency in autism. *BMC Medicine*, 7(1):62, 12 2009.

[8] Suma Jacob, Camille W Brune, C.S. Carter, Bennett L Leventhal, Catherine Lord, and Edwin H Cook. Association of the oxytocin receptor gene (OXTR) in Caucasian children and adolescents with autism. *Neuroscience Letters*, 417(1):6–9, 4 2007.

[9] Jonathan Sebat, B Lakshmi, Dheeraj Malhotra, Jennifer Troge, Christa Lese-Martin, Tom Walsh, Boris Yamrom, Seungtai Yoon, Alex Krasnitz, Jude Kendall, Anthony Leotta, Deepa Pai, Ray Zhang, Y.-H. Lee, James Hicks, Sarah J Spence, Annette T Lee, Kaija Puura, T. Lehtimaki, David Ledbetter, Peter K Gregersen, Joel Bregman, James S Sutcliffe, Vaidehi Jobanputra, Wendy Chung, D. Warburton, M.-C. King, D. Skuse, D. H. Geschwind, T. C. Gilliam, Kenny Ye, and Michael Wigler. Strong Association of De Novo Copy Number Mutations with Autism. *Science*, 316(5823):445–449, 4 2007.

[10] L. M. Hernandez, K. Krasileva, S. A. Green, L. E. Sherman, C. Ponting, R. McCarron, J. K. Lowe, D. H. Geschwind, S. Y. Bookheimer, and M. Dapretto. Additive effects of oxytocin receptor gene polymorphisms on reward circuitry in youth with autism. *Molecular psychiatry*, 22(8):1134–1139, 8 2017.

[11] Elissar Andari, J.-R. Duhamel, Tiziana Zalla, Evelyn Herbrecht, Marion Leboyer, and Angela Sirigu. Promoting social behavior with oxytocin in high-functioning autism spectrum disorders. *Proceedings of the National Academy of Sciences*, 107(9):4389–4394, 3 2010.

[12] Leeanne Green, Deborah Fein, Charlotte Modahl, Carl Feinstein, Lynn Waterhouse, and Mariana Morris. Oxytocin and autistic disorder: alterations in peptide forms. *Biological Psychiatry*, 50(8):609–613, 10 2001.

[13] Charlotte Modahl, Leeanne Green, Deborah Fein, Mariana Morris, Lynn Waterhouse, Carl Feinstein, and Harriet Levin. Plasma Oxytocin Levels in Autistic Children. *Biol Psychiatry*, 43:270–277, 1998.

[14] Mariaelvina Sala, Daniela Braida, Daniela Lentini, Marta Busnelli, Elisabetta Bulgheroni, Valeria Capurro, Annamaria Finardi, Andrea Donzelli, Linda Pattini, Tiziana Rubino, Daniela Parolaro, Katsuhiko Nishimori, Marco Parenti, and Bice Chini. Pharmacologic Rescue of Impaired Cognitive Flexibility, Social Deficits,

Increased Aggression, and Seizure Susceptibility in Oxytocin Receptor Null Mice: A Neurobehavioral Model of Autism. *Biological Psychiatry*, 69(9):875–882, 5 2011.

[15] Brian L Teng, Randal J Nonneman, Kara L Agster, Viktoriya D Nikolova, Tamara T Davis, Natallia V Riddick, Lorinda K Baker, Cort A Pedersen, Michael B Jarstfer, and Sheryl S Moy. Prosocial effects of oxytocin in two mouse models of autism spectrum disorders. *Neuropharmacology*, 72:187–196, 2013.

[16] Olga Peñagarikano, María T. Lázaro, Xiao-Hong Lu, Aaron Gordon, Hongmei Dong, Hoa A. Lam, Elior Peles, Nigel T. Maidment, Niall P. Murphy, X. William Yang, Peyman Golshani, and Daniel H. Geschwind. Exogenous and evoked oxytocin restores social behavior in the Cntnap2 mouse model of autism. *Science Translational Medicine*, 7(271):8–271, 1 2015.

[17] Huiping Huang, Caterina Michetti, Marta Busnelli, Francesca Managò, Sara Sannino, Diego Scheggia, Luca Giancardo, Diego Sona, Vittorio Murino, Bice Chini, and others. Chronic and acute intranasal oxytocin produce divergent social effects in mice. *Neuropsychopharmacology*, 39(5):1102–1114, 2014.

[18] Inga D. Neumann, Rodrigue Maloumby, Daniela I. Beiderbeck, Michael Lukas, and Rainer Landgraf. Increased brain and plasma oxytocin after nasal and peripheral administration in rats and mice. *Psychoneuroendocrinology*, 38(10):1985–1993, 10 2013.

[19] Christine Ecker. The neuroanatomy of autism spectrum disorder: An overview of structural neuroimaging findings and their translatability to the clinical setting. *Autism*, 21(1):18–28, 1 2017.

[20] Jeffrey A Engelman, Liang Chen, Xiaohong Tan, Katherine Crosby, Alexander R Guimaraes, Rabi Upadhyay, Michel Maira, Kate McNamara, Samanthi A Perera, Youngchul Song, Lucian R Chirieac, Ramneet Kaur, Angela Lightbown, Jessica Simendinger, Timothy Li, Robert F Padera, Carlos García-Echeverría, Ralph Weissleder, Umar Mahmood, Lewis C Cantley, and Kwok-Kin Wong. Effective use of PI3K and MEK inhibitors to treat mutant Kras G12D and PIK3CA H1047R murine lung cancers. *Nature Medicine*, 14(12):1351–1356, 12 2008.

[21] Michal Hrdlicka, Iva Dudova, Irena Beranova, Jiri Lisy, Tomas Belsan, Jiri Neuwirth, Vladimir Komarek, Ludvika Faladova, Marketa Havlovicova, Zdenek Sedlacek, Marek Blatny, and Tomas Urbanek. Subtypes of autism by cluster analysis based on structural MRI data. *European Child & Adolescent Psychiatry*, 14(3):138–144, 6 2005.

[22] Boris C. Bernhardt, Adriana Di Martino, Sofie L. Valk, and Gregory L. Wallace. Neuroimaging-Based Phenotyping of the Autism Spectrum. In *Current Topics in Behavioral Neurosciences*, volume 30, pages 341–355. Springer Verlag, 2016.

[23] Seok-Jun Hong, Sofie L Valk, Adriana Di Martino, Michael P Milham, and Boris C Bernhardt. Multidimensional Neuroanatomical Subtyping of Autism Spectrum Disorder. *Cerebral Cortex*, 28(10):3578–3588, 10 2018.

[24] Azadeh Kushki, Evdokia Anagnostou, Christopher Hammill, Pierre Duez, Jessica Brian, Alana Iaboni, Russell Schachar, Jennifer Crosbie, Paul Arnold, and Jason P. Lerch. Examining overlap and homogeneity in ASD, ADHD, and OCD: a data-driven, diagnosis-agnostic approach. *Translational Psychiatry*, 9(1):1–11, 12 2019.

[25] Jason P. Lerch, John G. Sled, and R. Mark Henkelman. *MRI Phenotyping of Genetically Altered Mice*, volume 711. Humana Press, Totowa, NJ, 2011.

[26] X. Josette Chen and Brian J. Nieman. Mouse Phenotyping with MRI. In Leif Schröder and Cornelius Faber, editors, *Methods in Molecular Biology*, volume 771, pages 595–631. Humana Press, Totowa, NJ, 2011.

[27] Kamila U Szulc, Jason P Lerch, Brian J Nieman, Benjamin B Bartelle, Miriam Friedel, Giselle A Suero-Abreu, Charles Watson, Alexandra L Joyner, and Daniel H Turnbull. 4D MEMRI atlas of neonatal FVB/N mouse brain development HHS Public Access. *Neuroimage*, 118:49–62, 2015.

[28] Brian J. Nieman, Matthijs C. van Eede, Shoshana Spring, Jun Dazai, R. Mark Henkelman, and Jason P. Lerch. MRI to Assess Neurological Function. *Current Protocols in Mouse Biology*, 8(2):e44, 6 2018.

[29] Brian J. Nieman, Jason P. Lerch, Nicholas A. Bock, X. Josette Chen, John G. Sled, and R. Mark Henkelman. Mouse behavioral mutants have neuroimaging abnormalities. *Human Brain Mapping*, 28(6):567–575, 6 2007.

[30] Jacob Ellegood, Brooke A. Babineau, R. Mark Henkelman, Jason P. Lerch, and Jacqueline N. Crawley. Neuroanatomical analysis of the BTBR mouse model of autism using magnetic resonance imaging and diffusion tensor imaging. *NeuroImage*, 70:288–300, 4 2013.

[31] Christoph Anacker, Jan Scholz, Kieran J. O'Donnell, Rylan Allemang-Grand, Josie Diorio, Rosemary C Bagot, Eric J Nestler, René Hen, Jason P Lerch, and Michael J Meaney. Neuroanatomic Differences Associated With Stress Susceptibility and Resilience. *Biological Psychiatry*, 79(10):840–849, 5 2016.

[32] Dulcie Vousden. *Whole brain imaging of learning, memory, and plasticity*. PhD thesis, University of Toronto, 2018.

[33] Tie-Yuan Zhang, Christopher L Keown, Xianglan Wen, Junhao Li, Dulcie A Vousden, Christoph Anacker, Urvashi Bhattacharyya, Richard Ryan, Josie Diorio, Nicholas O'Toole, Jason P Lerch, Eran A Mukamel, and Michael J Meaney. Environmental enrichment increases transcriptional and epigenetic differentiation between mouse dorsal and ventral dentate gyrus. *Nature Communications*, 9(1):298, 12 2018.

[34] Hanbing Lu, Z.-X. Xi, Leah Gitajn, William Rea, Yihong Yang, and Elliot A Stein. Cocaine-induced brain activation detected by dynamic manganese-enhanced magnetic resonance imaging (MEMRI). *Proceedings of the National Academy of Sciences*, 104(7):2489–2494, 2 2007.

[35] Anne L Wheeler, Jason P Lerch, M Mallar Chakravarty, Miriam Friedel, John G Sled, Paul J Fletcher, Sheena A Josselyn, and Paul W Frankland. Adolescent Cocaine Exposure Causes Enduring Macroscale Changes in Mouse Brain Structure. *Journal of Neuroscience*, 33(5):1797–1803, 1 2013.

[36] Mateusz Dudek, Usama Abo-Ramadan, Derik Hermann, Matthew Brown, Santiago Canals, Wolfgang H. Sommer, and Petri Hyytiä. Brain activation induced by voluntary alcohol and saccharin drinking in rats assessed with manganese-enhanced magnetic resonance imaging. *Addiction Biology*, 20(6):1012–1021, 11 2015.

[37] Shane A Perrine, Farhad Ghoddoussi, Kirtan Desai, Robert J Kohler, Ajay T Eapen, Michael J Lisieski, Mariana Angoa-Perez, Donald M Kuhn, Kelly E Bosse, Alana C Conti, David Bissig, and Bruce A Berkowitz. Cocaine-induced locomotor sensitization in rats correlates with nucleus accumbens activity on manganese-enhanced MRI HHS Public Access activity in freely behaving animals and to guide new calcium channel-based therapies for treating cocaine abuse and depe. *NMR Biomed*, 28(11):1480–1488, 2015.

[38] Jan Scholz, Yosuke Niibori, Paul W Frankland, and Jason P Lerch. Rotarod training in mice is associated with changes in brain structure observable with multimodal MRI. *NeuroImage*, 107:182–189, 2 2015.

[39] Mateusz Dudek, Santiago Canals, Wolfgang H Sommer, and Petri Hyytiä. Modulation of nucleus accumbens connectivity by alcohol drinking and naltrexone in alcohol-preferring rats: A manganese-enhanced magnetic resonance imaging study. *European Neuropsychopharmacology*, 26(3):445–455, 3 2016.

[40] Aditya N Bade, Howard E Gendelman, Michael D Boska, and Yutong Liu. MEMRI is a biomarker defining nicotine-specific neuronal responses in subregions of the rodent brain. *Am J Transl Res*, 9(2):601–610, 2017.

[41] Ellen van der Plas, T. Leigh Spencer Noakes, Darci T. Butcher, Rosanna Weksberg, Laura Galin-Corini, Elizabeth A. Wanstall, Patrick Te, Laura Hopf, Sharon Guger, Brenda J. Spiegler, Johann Hitzler, Russell J. Schachar, Shinya Ito, and Brian J. Nieman. Quantitative MRI outcomes in child and adolescent leukemia survivors: Evidence for global alterations in gray and white matter. *NeuroImage: Clinical*, 28:102428, 1 2020.

[42] G. Horev, J. Ellegood, J. P. Lerch, Y.-E. E. Son, L. Muthuswamy, H. Vogel, A. M. Krieger, A. Buja, R. M. Henkelman, M. Wigler, and A. A. Mills. Dosage-dependent phenotypes in models of 16p11.2 lesions found in autism. *Proceedings of the National Academy of Sciences*, 108(41):17076–17081, 10 2011.

[43] Cathy Bakker, Coleta Verheij, and et al. Fmr1 knockout mice: A model to study fragile X mental retardation. *Cell*, 78(1):23–33, 7 1994.

[44] Ozlem Bozdagi, Takeshi Sakurai, Danae Papapetrou, Xiaobin Wang, Dara L. Dickstein, Nagahide Takahashi, Yuji Kajiwara, Mu Yang, Adam M. Katz, Maria Luisa Scattoni, and others. Haploinsufficiency of the autism-associated Shank3 gene leads to deficits in synaptic function, social interaction, and social communication. *Mol Autism*, 1(1):15–15, 2010.

[45] K L Bales, M Solomon, S Jacob, J N Crawley, J L Silverman, R H Larke, E Sahagun, K R Puhger, M C Pride, and S P Mendoza. Long-term exposure to intranasal oxytocin in a mouse autism model. *Translational Psychiatry*, 4(11):e480, 11 2014.

[46] R Core Team. R: A Language and Environment for Statistical Computing, 2017.

[47] Jose Pinheiro and Douglas Bates. *Mixed-Effects Models in S and S-PLUS*. Springer, 2000.

[48] Douglas Bates, Martin Mächler, Ben Bolker, and Steve Walker. Fitting Linear Mixed-Effects Models Using lme4. *Journal of Statistical Software*, 67(1):1–48, 2015.

[49] Dulcie A Vousden, Elizabeth Cox, Rylan Allemang-Grand, Christine Lalibert E, Lily R Qiu, Zsuzsa Lindenmaier, Brian J Nieman, and Jason P Lerch. Continuous manganese delivery via osmotic pumps for manganese-enhanced mouse MRI does not impair spatial learning but leads to skin ulceration. *NeuroImage*, 173:411–420, 2018.

[50] Lily R Qiu, Darren J Fernandes, Kamila U Szulc-Lerch, Jun Dazai, Brian J Nieman, Daniel H Turnbull, Jane A Foster, Mark R Palmert, and Jason P Lerch. Mouse MRI shows brain areas relatively larger in males emerge before those larger in females. *Nature Communications*, 9(1):2615, 12 2018.

[51] Christopher R. Genovese, Nicole A Lazar, and Thomas Nichols. Thresholding of Statistical Maps in Functional Neuroimaging Using the False Discovery Rate. *NeuroImage*, 15(4):870–878, 4 2002.

[52] Jill L. Silverman, Mu Yang, Catherine Lord, and Jacqueline N. Crawley. Behavioural phenotyping assays for mouse models of autism. *Nature Reviews Neuroscience*, 11(7):490–502, 7 2010.

[53] Jacqueline N. Crawley. *What's wrong with my mouse?: behavioral phenotyping of transgenic and knockout mice*. Wiley-Interscience, Hoboken, N.J, 2nd ed edition, 2007.

[54] A Elizabeth De Guzman, Michael D Wong, Jacqueline A Gleave, and Brian J Nieman. Variations in post-perfusion immersion fixation and storage alter MRI measurements of mouse brain morphometry. *NeuroImage*, 142:687–695, 2016.

[55] Lindsay S. Cahill, Christine L. Laliberté, Jacob Ellegood, Shoshana Spring, Jacqueline A. Gleave, Matthijs C. van Eede, Jason P. Lerch, and R. Mark Henkelman. Preparation of fixed mouse brains for MRI. *NeuroImage*, 60(2):933–939, 4 2012.

[56] T. Leigh Spencer Noakes, R. Mark Henkelman, and Brian J. Nieman. Partitioning k-space for cylindrical three-dimensional rapid acquisition with relaxation enhancement imaging in the mouse brain. *NMR in Biomedicine*, 30(11):e3802, 11 2017.

[57] D L Collins, P Neelin, T M Peters, and A C Evans. Automatic 3D intersubject registration of MR volumetric data in standardized Talairach space. *Journal of computer assisted tomography*, 18(2):192–205, 1994.

[58] B Avants, C Epstein, M Grossman, and J Gee. Symmetric diffeomorphic image registration with cross-correlation: Evaluating automated labeling of elderly and neurodegenerative brain. *Medical Image Analysis*, 12(1):26–41, 2 2008.

[59] Brian B Avants, Nicholas J Tustison, Gang Song, Philip A Cook, Arno Klein, and James C Gee. A reproducible evaluation of ANTs similarity metric performance in brain image registration. *NeuroImage*, 54(3):2033–2044, 2 2011.

[60] M Mallar Chakravarty, Patrick Steadman, Matthijs C Van Eede, Rebecca D Calcott, Victoria Gu, Philip Shaw, Armin Raznahan, D Louis Collins, and Jason P Lerch. Performing Label-Fusion-Based Segmentation Using Multiple Automatically Generated Templates HHS Public Access. *Hum Brain Mapp*, 34(10):2635–2654, 2013.

[61] A.E. Dorr, J.P. Lerch, S Spring, N Kabani, and R.M. Henkelman. High resolution three-dimensional brain atlas using an average magnetic resonance image of 40 adult C57Bl/6J mice. *NeuroImage*, 42(1):60–69, 8 2008.

[62] Kay Richards, Charles Watson, Rachel F Buckley, Nyoman D Kurniawan, Zhengyi Yang, Marianne D Keller, Richard Beare, Perry F Bartlett, Gary F Egan, Graham J Galloway, George Paxinos, Steven Petrou, and David C Reutens. Segmentation of the mouse hippocampal formation in magnetic resonance images. *NeuroImage*, 58(3):732–740, 10 2011.

[63] Jeremy F.P. Ullmann, Charles Watson, Andrew L. Janke, Nyoman D. Kurniawan, and David C. Reutens. A segmentation protocol and MRI atlas of the C57BL/6J mouse neocortex. *NeuroImage*, 78:196–203, 9 2013.

[64] Patrick E. Steadman, Jacob Ellegood, Kamila U. Szulc, Daniel H. Turnbull, Alexandra L. Joyner, R. Mark Henkelman, and Jason P. Lerch. Genetic Effects on Cerebellar Structure Across Mouse Models of Autism Using a Magnetic Resonance Imaging Atlas. *Autism Research*, 7(1):124–137, 2 2014.

[65] Catherine Mankiw, Min Tae M. Park, P.K. Reardon, Ari M Fish, Liv S Clasen, Deanna Greenstein, Jay N Giedd, Jonathan D Blumenthal, Jason P Lerch, M. Mallar Chakravarty, and Armin Raznahan. Allometric Analysis Detects Brain Size-Independent Effects of Sex and Sex Chromosome Complement on Human Cerebellar Organization. *The Journal of Neuroscience*, 37(21):5221–5231, 5 2017.

[66] Alessandro Crippa, Giuseppe Del Vecchio, Silvia Busti Ceccarelli, Maria Nobile, Filippo Arrigoni, and Paolo Brambilla. Cortico-Cerebellar Connectivity in Autism Spectrum Disorder: What Do We Know So Far? *Frontiers in Psychiatry*, 7:20, 2 2016.

[67] Yawei Cheng, Kun-Hsien Chou, I-Yun Chen, Yang-Teng Fan, Jean Decety, and Ching-Po Lin. Atypical development of white matter microstructure in adolescents with autism spectrum disorders. *NeuroImage*, 50(3):873–882, 4 2010.

[68] S Hossein Fatemi, Kimberly A Aldinger, Paul Ashwood, Margaret L Bauman, Charles D Blaha, Gene J Blatt, Abha Chauhan, Ved Chauhan, Stephen R Dager, Price E Dickson, Annette M Estes, Dan Goldowitz, Detlef H Heck, Thomas L Kemper, Bryan H King, Loren A Martin, Kathleen J Millen, Guy Mittleman,

Matthew W Mosconi, Antonio M Persico, John A Sweeney, Sara J Webb, John P Welsh, and Hossein Fatemi. Consensus Paper: Pathological Role of the Cerebellum in Autism. *Cerebellum*, 11(3):777–807, 2012.

[69] Peter T Tsai, Yunxiang Chu, Emily Greene-Colozzi, Abbey R Sadowski, Jarrett M Leech, Jason Steinberg, Jacqueline N Crawley, Wade G Regehr, and Mustafa Sahin. Autistic-like behavior and cerebellar dysfunction in Purkinje cell Tsc1 mutant mice HHS Public Access. *Nature*, 488(7413):647–651, 2012.

[70] Brian N Mathur. The claustrum in review. *Frontiers in Systems Neuroscience*, 8, 4 2014.

[71] Caroline E. Robertson and Simon Baron-Cohen. Sensory perception in autism, 2017.

[72] Shawn F. Sorrells, Mercedes F. Paredes, Arantxa Cebrian-Silla, Kadellyn Sandoval, Dashi Qi, Kevin W. Kelley, David James, Simone Mayer, Julia Chang, Kurtis I. Auguste, Edward F. Chang, Antonio J. Gutierrez, Arnold R. Kriegstein, Gary W. Mathern, Michael C. Oldham, Eric J. Huang, Jose Manuel Garcia-Verdugo, Zhengang Yang, and Arturo Alvarez-Buylla. Human hippocampal neurogenesis drops sharply in children to undetectable levels in adults. *Nature*, 555(7696):377–381, 3 2018.

[73] Ratan D Bhardwaj, Maurice A Curtis, Kirsty L Spalding, Bruce A Buchholz, David Fink, T. Bjork-Eriksson, Claes Nordborg, Fred H Gage, Henrik Druid, Peter S Eriksson, and J. Frisen. Neocortical neurogenesis in humans is restricted to development. *Proceedings of the National Academy of Sciences*, 103(33):12564–12568, 8 2006.

[74] Alvaro Pascual-Leone, Catarina Freitas, Lindsay Oberman, Jared C Horvath, Mark Halko, Mark Eldaief, Shahid Bashir, Marine Vernet, Mouhshin Shafi, Brandon Westover, Andrew M Vahabzadeh-Hagh, and Alexander Rotenberg. Characterizing Brain Cortical Plasticity and Network Dynamics Across the Age-Span in Health and Disease with TMS-EEG and TMS-fMRI. *Brain Topogr*, 24:3–4, 2011.

[75] Gareth Leng and Mike Ludwig. Intranasal Oxytocin: Myths and Delusions. *Biological Psychiatry*, 79(3):243–250, 2 2016.